

# UC Davis

## UC Davis Previously Published Works

### Title

Selective Photochemical Oxidation of Reduced Dissolved Organic Sulfur to Inorganic Sulfate.

### Permalink

<https://escholarship.org/uc/item/3j75r4wn>

### Journal

Environmental science & technology letters, 10(6)

### ISSN

2328-8930

### Author

Poulin, Brett A

### Publication Date

2023-06-01

### DOI

10.1021/acs.estlett.3c00210

### Copyright Information

This work is made available under the terms of a Creative Commons Attribution License, available at <https://creativecommons.org/licenses/by/4.0/>

Peer reviewed

# Selective Photochemical Oxidation of Reduced Dissolved Organic Sulfur to Inorganic Sulfate

Brett A. Poulin\*



Cite This: *Environ. Sci. Technol. Lett.* 2023, 10, 499–505



Read Online

ACCESS |



Metrics & More



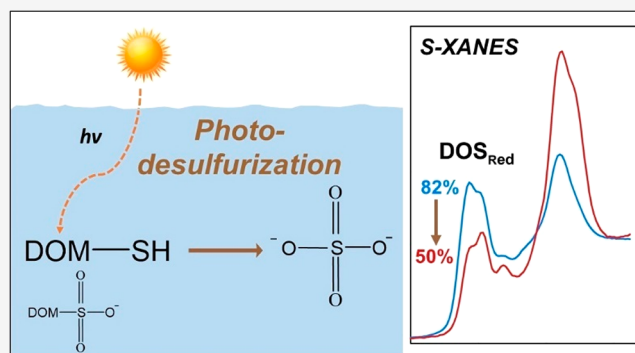
Article Recommendations



Supporting Information

**ABSTRACT:** The chemical nature and stability of reduced dissolved organic sulfur ( $\text{DOS}_{\text{Red}}$ ) have implications on the biogeochemical cycling of trace and major elements across fresh and marine aquatic environments, but the underlying processes governing  $\text{DOS}_{\text{Red}}$  stability remain obscure. Here, dissolved organic matter (DOM) was isolated from a sulfidic wetland, and laboratory experiments quantified dark and photochemical oxidation of  $\text{DOS}_{\text{Red}}$  using atomic-level measurement of sulfur X-ray absorption near-edge structure (XANES) spectroscopy.  $\text{DOS}_{\text{Red}}$  was completely resistant to oxidation by molecular oxygen in the dark and underwent rapid and quantitative oxidation to inorganic sulfate ( $\text{SO}_4^{2-}$ ) in the presence of sunlight. The rate of  $\text{DOS}_{\text{Red}}$  oxidation to  $\text{SO}_4^{2-}$  greatly exceeded that of DOM photomineralization, resulting in a 50% loss of total DOS and 78% loss of  $\text{DOS}_{\text{Red}}$  over 192 h of irradiance. Sulfonates ( $\text{DOS}_{\text{SO}_3}$ ) and other minor oxidized DOS functionalities were not susceptible to photochemical oxidation. The observed susceptibility of  $\text{DOS}_{\text{Red}}$  to photodesulfurization, which has implications on carbon, sulfur, and mercury cycling, should be comprehensively evaluated across diverse aquatic environments of differing DOM composition.

**KEYWORDS:** Dissolved organic sulfur, Desulfurization, DOM photochemistry, S-XANES



## INTRODUCTION

Dissolved organic sulfur (DOS) is a dynamic constituent of fresh<sup>1</sup> and marine waters<sup>2,3</sup> that influences diverse biogeochemical processes, including the cycling of sulfur (S) between organic and inorganic forms,<sup>1</sup> formation of atmospheric organic S species (e.g., carbonyl sulfide (COS), carbonyl disulfide (CS<sub>2</sub>), and dimethyl sulfide (DMS)),<sup>4</sup> and transport,<sup>5</sup> bioavailability,<sup>6</sup> and photochemical reactivity of mercury (Hg).<sup>7,8</sup> The abiotic sulfuration of dissolved organic matter (DOM), involving nucleophilic addition of inorganic sulfide into DOM as reduced DOS ( $\text{DOS}_{\text{Red}}$ ) (namely, thiols),<sup>1,3,9</sup> occurs in wastewater treatment systems,<sup>10</sup> wetlands<sup>1</sup> and estuaries,<sup>11</sup> sulfidic lakes,<sup>12</sup> and diverse marine waters.<sup>13–15</sup> Aside from thiols,  $\text{DOS}_{\text{Red}}$  can be present as thioethers, disulfides, and perhaps thiophenes.<sup>3,16</sup> Low-molecular-weight thiols (e.g., cysteine, glutathione) rapidly oxidize in dark and light oxic conditions,<sup>17,18</sup> whereas  $\text{DOS}_{\text{Red}}$  is abundant, ranging from 50 to 70% of total DOS in freshwaters.<sup>1,16,19</sup> Concentrations of  $\text{DOS}_{\text{Red}}$  exceed low-molecular-weight thiols by 2–3 orders of magnitude.<sup>20</sup> Therefore, understanding the stability of DOS is central to ascertaining the implications of DOS chemistry on the above-mentioned biogeochemical processes. To date, no studies have quantified the atomic-level transformation of  $\text{DOS}_{\text{Red}}$  due to dark and light oxidation, as research has probed photochemical changes in low-

molecular-weight thiols<sup>17,21,22</sup> or total DOS loss,<sup>23–25</sup> or formation of organic and inorganic byproducts.<sup>4,21</sup>

Here, the stability of  $\text{DOS}_{\text{Red}}$  to light and dark oxidation was quantified by atomic measurements of S X-ray absorption spectroscopy, which quantifies different DOS oxidation states. DOM was isolated from a sulfidic wetland known to have high  $\text{DOS}_{\text{Red}}$ <sup>1</sup> and subjected to laboratory oxidation by O<sub>2</sub> in the dark and artificial sunlight. Quantified changes in the DOM S content, DOS oxidation states, and inorganic S byproducts provide a more complete assessment of the stability of  $\text{DOS}_{\text{Red}}$  in aquatic environments.

## MATERIALS AND METHODS

**DOM Sample Collection and Extraction.** DOM was isolated from a representative sulfidic freshwater environment for laboratory experimentation as shown in Figure S1 and detailed in Section S1 of the Supporting Information (SI). Briefly, pore water was collected from a sulfidic Florida

Received: March 21, 2023

Revised: April 26, 2023

Accepted: April 26, 2023

Published: May 3, 2023



**Table 1. Data of Oxidation Experiments Including the Duration, Atomic Sulfur-to-Carbon Ratio (S/C) of Dissolved Organic Matter (DOM), Concentrations and Percentages of DOS Atomic Fractions, Inorganic Sulfate (SO<sub>4</sub><sup>2-</sup>), and Total Sulfur (S<sub>Tot</sub>)**

Sample	Exp. Duration <sup>a</sup>	[DOC] mgC L <sup>-1</sup>	DOM Atomic S/C <sup>b</sup>	DOS Species by S K-edge XANES Spectroscopy <sup>b,c</sup>						[SO <sub>4</sub> <sup>2-</sup> ] <sup>d</sup> μM	S <sub>Tot</sub> <sup>e</sup> μM
				DOS <sub>Red</sub> μM	DOS <sub>Sulf</sub> μM	DOS <sub>SO<sub>2</sub></sub> μM	DOS <sub>SO<sub>3</sub></sub> μM	DOS <sub>SO<sub>4</sub></sub> μM	(%)		
t = 0 (initial)	—	37.9	9.6 × 10 <sup>-3</sup>	24.6 (82%)	0.2 (0.8%)	0.7 (2.4%)	3.6 (12%)	0.9 (2.9%)	1.0	31.2 (—)	
Dark, Anoxic Control	336 h	38.6	9.7 × 10 <sup>-3</sup>	24.2 (77%)	0.5 (1.5%)	0.9 (2.8%)	4.0 (13%)	1.8 (5.8%)	2.8	34.1 (110%)	
Dark O <sub>2</sub> Purge	192 h 30 mL min <sup>-1</sup>	37.8	9.0 × 10 <sup>-3</sup>	22.4 (79%)	0.3 (1.2%)	0.8 (2.7%)	3.7 (13%)	1.0 (3.5%)	2.8	30.9 (99%)	
Light-1	1.3 h	35.0	9.4 × 10 <sup>-3</sup>	21.0 (77%)	0.5 (1.8%)	0.8 (2.9%)	3.8 (14%)	1.4 (5.1%)	2.9	30.3 (97%)	
Light-2	5.3 h	34.4	8.8 × 10 <sup>-3</sup>	18.4 (73%)	0.5 (2.2%)	0.8 (3.3%)	3.8 (15%)	1.6 (6.2%)	4.0	29.1 (93%)	
Light-3	24 h	32.6	7.6 × 10 <sup>-3</sup>	14.0 (68%)	0.7 (3.2%)	0.8 (3.7%)	3.7 (18%)	1.6 (7.9%)	8.5	29.2 (94%)	
Light-3 (replicate)	24 h	33.1	7.9 × 10 <sup>-3</sup>	15.2 (69%)	0.8 (3.5%)	0.7 (3.4%)	3.9 (18%)	1.3 (6.0%)	8.1	30.0 (96%)	
Light-4	78 h	28.4	6.1 × 10 <sup>-3</sup>	8.4 (58%)	0.5 (3.1%)	0.7 (4.9%)	3.0 (21%)	2.0 (14%)	14.0	28.5 (91%)	
Light-5	192 h	27.0	4.9 × 10 <sup>-3</sup>	5.5 (50%)	0.4 (3.7%)	0.6 (5.6%)	3.1 (28%)	1.5 (13%)	21.8	32.9 (106%)	

<sup>a</sup>For light treatment samples the experimental duration is the time in a solar simulator at 500 W m<sup>-2</sup>. <sup>b</sup>Measured on DOM extracts. <sup>c</sup>Eq 2 used to determine aqueous concentrations. Values in parentheses are atomic fractions (%) of organic sulfur. <sup>d</sup>Measured on aqueous solutions prior to DOM extraction. <sup>e</sup>Eq 3 used to determine total S concentration.

Everglades wetland (site WCA 2A-O; 26.42506°N, -80.47601°W) where DOS<sub>Red</sub> is elevated,<sup>1</sup> stored under N<sub>2</sub> at 4 °C, and shipped on ice to the U.S. Geological Survey (Boulder, Colorado) for DOM isolation. The pore water was characterized in the field for pH (6.62), oxidation–reduction potential (–252 mV), dissolved oxygen (0.11 mg L<sup>-1</sup>), and sulfide (0.22 mM), and via laboratory measurements of dissolved organic carbon (DOC) (42.7 mgC L<sup>-1</sup>) and sulfate concentration (0.38 mM), and DOM specific ultraviolet absorbance at 254 nm (SUVA<sub>254</sub>) (3.4 L (mg m)<sup>-1</sup>).<sup>26</sup> In the laboratory, residual inorganic sulfide was removed by purging with helium at pH 4.0, and the hydrophobic organic acid (HPOA) fraction of DOM was isolated on XAD-8 resin<sup>27</sup> using trace-metal grade acids, degassed solutions, and N<sub>2</sub>-flushed tubing. An experiment (outlined in Section S2 of the SI) evaluated the oxidation of DOS during the elution step by comparing DOM isolated by XAD-8 resin (base elution) to PPL resin (methanol elution)<sup>28</sup> and verified that DOM isolated by XAD-8 resin using deaerated solutions did not result in measurable oxidation of DOS (Figure S2, Tables S1–S2). The HPOA fraction accounted for 54% of the whole water DOC and was stored for up to 21 days (pH 3.5, under N<sub>2</sub>, 4 °C) for use in laboratory experiments.

**Laboratory Oxidation Experiments.** The purified DOM sample was diluted with deaerated high-purity water (≥18 MΩ cm; Barnstead GenPro UV) to a DOC concentration of 37.9 mgC L<sup>-1</sup> (pH 7) (complete details in SI and Figure S1), similar to surface waters of sulfate-enriched wetlands<sup>1,12,26</sup> but lower than those in previous DOS photolysis studies.<sup>21</sup> Although no pH buffer was used, subtle changes in pH expected from light exposure<sup>29</sup> were not expected to dramatically influence the DOS photochemical oxidation rates.<sup>17</sup> The initial DOM was sampled for characterization (termed t = 0 (Initial)). The following three experimental treatments were performed in 2 L quartz round-bottom flasks with 1 L of DOM solution (Figure S3a); the large volume was necessary for DOS characterization with this

technique.<sup>1</sup> (1) A dark anoxic control treatment (*n* = 1, termed Dark, Anoxic Control) was stored in the dark, under N<sub>2</sub> at 22 ± 2 °C for 14 d to identify changes in DOS during storage or DOM reisolation. (2) A dark O<sub>2</sub> purge treatment (*n* = 1, termed Dark, O<sub>2</sub> Purge) quantified oxidation of DOS by O<sub>2</sub> and was purged in the dark with zero-grade air for 192 h (20.5% O<sub>2</sub>, 79.5% N<sub>2</sub>; 30 mL min<sup>-1</sup>; 22 ± 2 °C). (3) The light treatment (termed Light 1–5 with one data point collected in duplicate, *n* = 6) was performed in a temperature-controlled solar simulator (Suntest XLS) at 500 W m<sup>-2</sup> and 30 °C (300–800 nm irradiance range, spectrum provided in Figure S3b). Immediately before irradiation, DOM solutions were oxygen-saturated by purging with zero-grade air (98% saturation; an Orion RDO optical probe). Independent vessels were irradiated for 1.3, 5.3, 24 (*n* = 2), 78, and 192 h. Light treatments of 24–192 h duration were purged with zero-grade air every 12 h to prevent the depletion of O<sub>2</sub>.<sup>21</sup>

Following dark and light oxidation experiments, experimental solutions were sampled for aqueous measurements including DOC concentration, DOM absorption, and fluorescence properties (decadic absorption coefficients at 254 nm ( $\alpha_{254}$ ) and 400 nm ( $\alpha_{400}$ ); SUVA<sub>254</sub>;<sup>30</sup> spectral slope from 275 to 295 nm ( $S_{275-295}$ ;  $\times 10^{-3}$  nm<sup>-1</sup>);<sup>31</sup> humification index (HIX)<sup>32</sup>), and sulfate (SO<sub>4</sub><sup>2-</sup>) and thiosulfate (S<sub>2</sub>O<sub>3</sub><sup>2-</sup>) concentration by ion chromatography. Complete information on these measurements is provided in Section S1 of the SI. DOM optical measurements were used to identify changes in the DOM composition.<sup>33</sup> Next, DOM solutions were deaerated and DOM was reisolated on XAD-8 resin (to remove inorganic S species), lyophilized, and stored under N<sub>2</sub> for DOS characterization.

**DOS Characterization.** Atomic S and C contents (and thus atomic S/C) of freeze-dried DOM samples were determined by Huffman Hazen Laboratories (Golden, CO) using International Humic Substances Society (IHSS) methods. Sulfur K-edge XANES spectra were collected on freeze-dried DOM samples

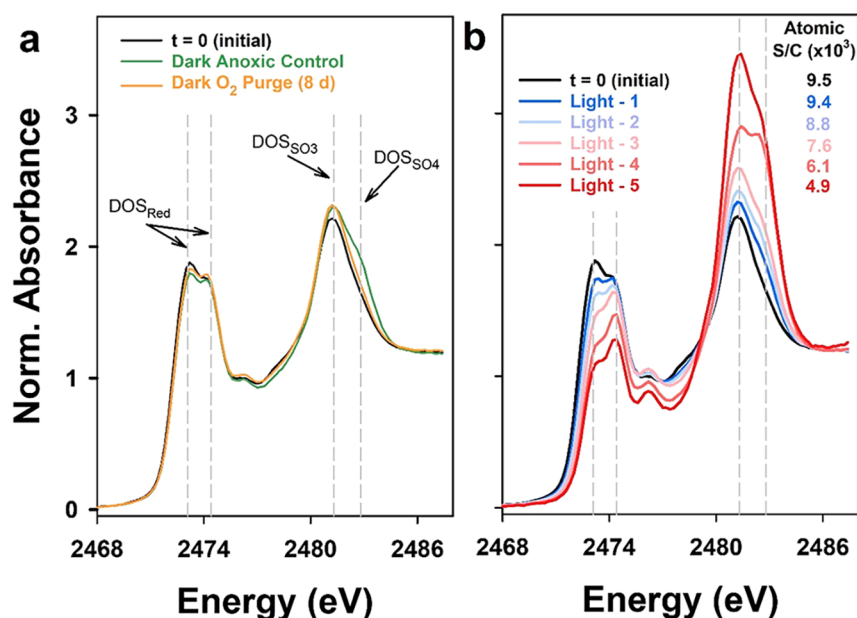


**Figure 1.** Sulfur K-edge XANES spectra comparing the DOM at the start of the experiment ( $t = 0$  (initial)) to (a) the Dark Anoxic control and Dark  $O_2$  Purge (192 h) treatments and (b) light treatment (Light 1–5, 1.3–192 h). Gray dashed vertical lines identify nominal energies of  $DOS_{Red}$  ( $E_0 = 2473.1$  and  $2474.4$  eV for exocyclic and heterocyclic reduced S), sulfonate ( $DOS_{SO_3}$ ,  $E_0 = 2481.3$  eV), and organosulfate ( $DOS_{SO_4}$ ,  $E_0 = 2482.8$  eV) functionalities. In subplot a, spectra show no considerable change in DOM sulfur functionalities in the Dark Anoxic control and Dark  $O_2$  Purge (192 h) treatments compared to the initial sample ( $t = 0$ ). In subplot b, spectra show a systematic decrease in the relative distribution of  $DOS_{Red}$  functionalities and an increase in the relative distribution of  $DOS_{SO_3}$  and  $DOS_{SO_4}$  with increased cumulative irradiance. The decrease in the relative distribution of  $DOS_{Red}$  functionalities is accompanied by a decrease in the atomic sulfur-to-carbon content (Atomic S/C) of the DOM. Gaussian decompositions of spectra and parameter values are provided in Figures S6 and S8 and Tables S3–S4.

(pressed as 5 mm pellets; see evaluation in Figure S4) on beamline 9-BM-B of the Advanced Photon Source (Argonne National Laboratory) as detailed previously<sup>1</sup> and in Section S1e. DOS atomic fractions ( $f_{DOS_x}$ ) were determined with a precision estimated at  $\leq 1.6\%$  (based on measurement of IHSS samples)<sup>16</sup> for exocyclic reduced ( $DOS_{Exo}$ ), heterocyclic reduced ( $DOS_{Hetero}$ ), sulfoxide ( $DOS_{Sulf}$ ), sulfone ( $DOS_{SO_2}$ ), sulfonate ( $DOS_{SO_3}$ ), and organosulfate ( $DOS_{SO_4}$ ). Nominal energies of  $DOS_{Exo}$  and  $DOS_{Hetero}$  are 2473.1 and 2474.4 eV, respectively, based on measurement of diverse model compounds.<sup>16</sup> However, S-XANES spectra of reduced S model compounds likely in DOM (e.g., thiols, thioethers, disulfide, and thiophenes) span the energy range of  $DOS_{Exo}$  and  $DOS_{Hetero}$  (Figure S5)<sup>16</sup> and cannot easily be resolved due to X-ray absorption doublets and shoulders. Thus, this study presents the total reduced  $DOS_{Red}$  defined in eq 1.

$$DOS_{Red} = DOS_{Exo} + DOS_{Hetero} \quad (1)$$

Concentrations of DOS functionalities, relative to carbon, were calculated by multiplying the fraction of each DOS functionality by the atomic S/C. Aqueous concentrations of DOS functionalities ( $[DOS_x]$ ) were calculated using eq 2, where  $[DOC]$  is the DOC concentration measured on experimental solutions before DOM reisolation and the atomic S/C and  $f_{DOS_x}$  are measured on DOM extracts.

$$[DOS_x] = [DOC] \times \text{atomic} \frac{S}{C} \times f_{DOS_x} \quad (2)$$

Total S concentration ( $S_{Tot}$ ) was determined using eq 3, where  $[DOC]$  and  $[SO_4^{2-}]$  are the DOC and  $SO_4^{2-}$  concentrations measured on experimental solutions before DOM reisolation, respectively, and the atomic S/C is of the DOM extract.

$$S_{Tot} = \left( [DOC] \times \text{atomic} \frac{S}{C} \right) + [SO_4^{2-}] \quad (3)$$

## RESULTS AND DISCUSSION

**Dark Stability of Dissolved Organic Sulfur.** DOM at the start of the experiment ( $t = 0$  (initial)) showed elevated organic S content (atomic S/C =  $9.6 \times 10^{-3}$ ; Table 1) and an S K-edge XANES spectrum (Figure 1a) with prominent absorption at energies of  $DOS_{Red}$  functionalities. The distribution of DOS functionalities, based on spectral fitting (Figure S6, Table S3), quantified that  $DOS_{Red}$  accounted for 82% of total DOS in the  $t = 0$  (initial) sample. Of the 82% of  $DOS_{Red}$ , approximately two-thirds was highly reduced  $DOS_{Exo}$  and one-third was  $DOS_{Hetero}$ . The concentration of  $DOS_{Red}$  in experimental solutions was  $24.6 \mu\text{M}$ , whereas inorganic  $SO_4^{2-}$  and  $S_2O_3^{2-}$  were minor components ( $1.0 \mu\text{M}$  and  $<0.45 \mu\text{M}$ , respectively). The high proportion of  $DOS_{Red}$  is consistent with previous investigations of sulfur-enriched Everglades wetlands<sup>1,34</sup> and peat that has undergone sulfurization<sup>35</sup> but higher than surface water DOM samples.<sup>16</sup> Previous measurements of DOM from this location concluded that abiotic sulfurization yields  $DOS_{Red}$  primarily as thiols and thioethers, based on complementary use of S K-edge XANES spectroscopy and ultrahigh resolution mass spectrometry.<sup>1</sup> Here,  $DOS_{Red}$  stability to dark oxidation was first evaluated under anoxic conditions (Dark Anoxic Control treatment) and by  $O_2$  (Dark  $O_2$  Purge treatment). The Dark Anoxic Control treatment, held anoxic for 14 days, exhibited minor differences in DOS content and functionality (atomic S/C =  $9.7 \times 10^{-3}$  and  $DOS_{Red} = 77\%$  of total DOS, respectively) compared to the  $t = 0$  (initial) sample (Figure 1a, Table 1); this confirms negligible oxidation of  $DOS_{Red}$  under anoxic storage or during DOM reisolation. The Dark  $O_2$  Purge treatment, purged

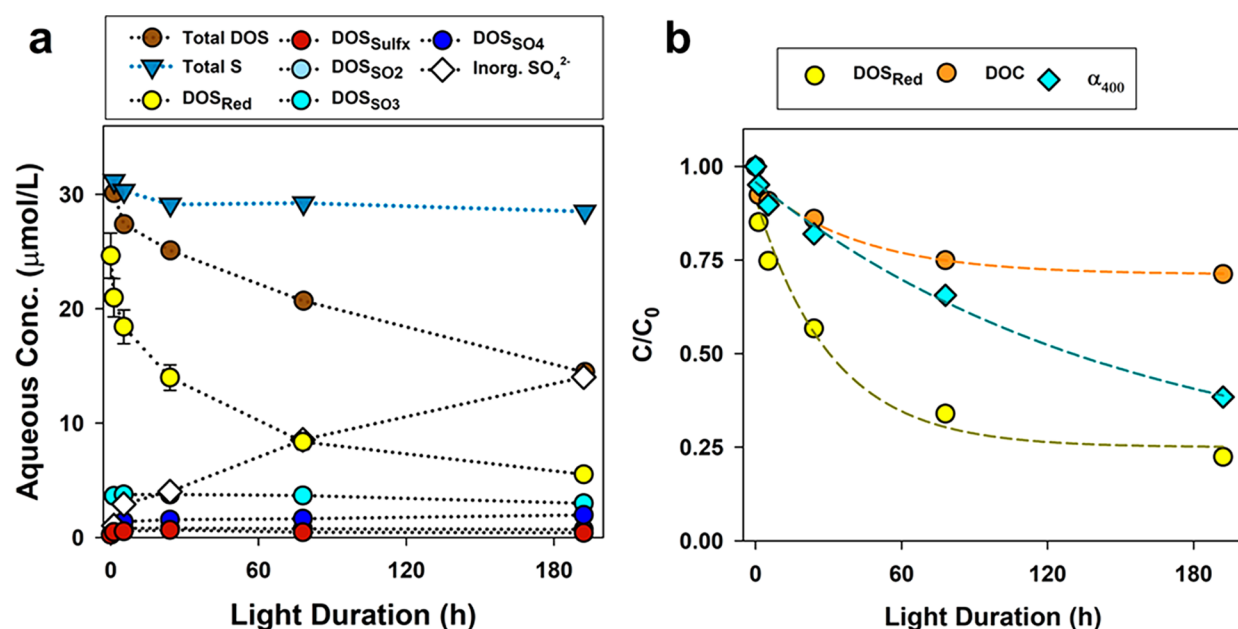


**Figure 2.** Kinetics results of light treatment (Light 1–5, 1.3–192 h) including the (a) aqueous concentrations of total sulfur (Total S), total organic sulfur (Total DOS), five DOS functionalities quantified by S K-edge XANES spectroscopy (DOS<sub>Red</sub>, DOS<sub>Sulfx</sub>, DOS<sub>SO2</sub>, DOS<sub>SO3</sub>, DOS<sub>SO4</sub>), and inorganic sulfate (SO<sub>4</sub><sup>2-</sup>). Plot of (b) C/C<sub>0</sub> showing the rapid rate of DOS<sub>Red</sub> photodegradation in comparison to DOC photomineralization and DOM photobleaching (shown as  $\alpha_{400}$ ). In plot (a), the decrease in concentrations of DOS<sub>Red</sub> functionalities with increasing light duration is concurrent with the increase in SO<sub>4</sub><sup>2-</sup> concentration; dotted lines are provided to guide the eye, and error bars present accuracies of DOS<sub>Red</sub>. In plot (b), the dashed lines present the exponential fit of the data to guide the eye.

for 8 days with zero-grade air, had similar DOS content (atomic S/C =  $9.0 \times 10^{-3}$ ), DOS speciation (DOS<sub>Red</sub> = 79%), and SO<sub>4</sub><sup>2-</sup> concentration (2.8  $\mu\text{M}$ ) as the  $t = 0$  (initial) sample. Differences in DOS<sub>Red</sub> abundance between these three DOM samples were small and within the accuracy of S K-edge XANES measurements,<sup>16</sup> and DOM had comparable DOS content (within 6.2%), DOC and SO<sub>4</sub><sup>2-</sup> concentrations, and DOM optical properties (Table 1, Figure S7). In summary, DOS<sub>Red</sub> was completely resistant to dark oxidation, consistent with experiments tracking reaction byproducts<sup>21</sup> and the observed stability of DOS to redox manipulations.<sup>36</sup>

#### Selective Photochemical Oxidation of Reduced DOS.

DOM exposure to artificial sunlight yielded systematic and pronounced changes in S K-edge XANES spectra (Figure 1b), atomic fractions of DOS functionalities (Figure S8, Table S4), and DOM S content (Table 1). With increasing cumulative irradiance (light 1–5, 1.3–192 h light exposure), systematic decreases were observed in X-ray absorption at energies of DOS<sub>Red</sub> functionalities. Fitting results quantified a systematic decrease in DOS<sub>Red</sub> from 82% of total DOS in the  $t = 0$  (initial) sample to 50% at 192 h of irradiance. An experimental replicate of the Light 3 sample confirmed good reproducibility for each DOS functionality (differences  $\leq 1.7\%$ ) (Figure S9, Tables 1 and S4). Simultaneously, a dramatic and systematic decrease was observed in the DOM S content (49% decrease in atomic S/C). Aqueous concentrations of DOS species (eq 2) show dramatic decreases in DOS<sub>Red</sub> with increasing cumulative irradiance (Figure 2a). In contrast, concentrations of other DOS functionalities (DOS<sub>Sulfx</sub>, DOS<sub>SO2</sub>, DOS<sub>SO3</sub>, and DOS<sub>SO4</sub>) were largely uniform in the light treatment. Decreases in DOS<sub>Red</sub> concentration accounted for all changes in the DOS<sub>Tot</sub> concentration (Figure S10), confirming that shifts in S K-edge XANES spectra and decreases in atomic S/C of DOM were exclusively due to the oxidation of DOS<sub>Red</sub>. The decrease in the

DOS<sub>Red</sub> concentration with increasing irradiance was mirrored by a quantitative increase in the SO<sub>4</sub><sup>2-</sup> concentration (from 1.0 to 21.8  $\mu\text{M}$ ; Figure 2a). Importantly, the DOS<sub>Red</sub> concentration approached an asymptote, with 37% of the DOS<sub>Tot</sub> being recalcitrant to photochemical oxidation over the experiment, similar to observations made of DOM from diverse sources.<sup>21</sup> A mass balance analysis of total S in the light experiment (S<sub>Tot</sub>; eq 3) accounted for 93–106% of S<sub>Tot</sub> at all time points (Table 1), verifying quantitative formation of SO<sub>4</sub><sup>2-</sup> concurrent with photochemical oxidation of DOS<sub>Red</sub>.

The light treatment also yielded systematic responses in the DOC concentration and DOM optical indices (Figure S7). Between the  $t = 0$  (initial) and Light 5 sample, the DOC concentration decreased from 37.9 to 27.0  $\text{mgC L}^{-1}$ ,  $\alpha_{254}$  and  $\alpha_{400}$  values decreased by 60%, and systemic shifts in DOM optical indices were observed including a decrease in DOM SUVA<sub>254</sub> (from 4.6 to 2.6  $\text{L (mgC m)}^{-1}$ ), increase in S<sub>275–295</sub> (from 14.9 to 16.8  $\times 10^{-3} \text{ nm}^{-1}$ ), and decrease in HIX (from 24.2 to 9.4) (Figure S7). These changes in DOC concentration and DOM optical metrics were strictly due to photochemical processes, consistent with previous observations of photomineralization<sup>21</sup> and photobleaching of DOM chromophores.<sup>31,33</sup>

Relative rates of photochemical transformations differed drastically between the DOS<sub>Red</sub> concentration, DOC concentration, and DOM absorption coefficients (e.g.,  $\alpha_{400}$ ), as shown in Figure 2b as C/C<sub>0</sub> versus light exposure. After 5.3 h of irradiance, 25% of the DOS<sub>Red</sub> was photo-oxidized to SO<sub>4</sub><sup>2-</sup> whereas  $\alpha_{400}$  and DOC concentration only decreased by 5% and 3%, respectively. After 192 h of irradiance, 78% of the DOS<sub>Red</sub> was photo-oxidized to SO<sub>4</sub><sup>2-</sup>. DOS<sub>Red</sub> oxidation rates could not be adequately modeled using first- or second-order reaction kinetics. The rapid decrease in relative concentration of DOS<sub>Red</sub> demonstrates the high susceptibility of the majority of DOS<sub>Red</sub>

groups to photochemical oxidation to  $\text{SO}_4^{2-}$ , notably faster than the photolysis of DOM chromophores and photomineralization of DOC.

The contrasting stability of  $\text{DOS}_{\text{Red}}$  to partial or complete oxidation under dark and light conditions, with little evidence of photochemical oxidation or accumulation of intermediate DOS species (e.g.,  $\text{DOS}_{\text{SO}_2}$ ,  $\text{DOS}_{\text{SO}_3}$ , and  $\text{DOS}_{\text{SO}_4}$ ), could be explained by specific  $\text{DOS}_{\text{Red}}$  chemistry or mechanisms of oxidative protection. At the start of the experiment,  $\text{DOS}_{\text{Red}}$  was likely present as a mixture of thiol and thioether groups, which both could originate from sulfurization reactions<sup>3,9</sup> or biomolecules (e.g., cysteine and methionine) and are known to undergo photochemical oxidation to  $\text{SO}_4^{2-}$ .<sup>21</sup> Previous measurements of DOM from this wetland confirmed that 98% of molecules that made up  $\text{DOS}_{\text{Red}}$  had one S atom (e.g.,  $\text{CHOS}_1$ ,  $\text{CHON}_{1-2}\text{S}_1$ ),<sup>1</sup> discounting the prominence of disulfide moieties. Further, thiols are confirmed in DOM from diverse aquatic environments including sulfidic wetlands and lakes, based on measured binding configuration<sup>37</sup> and strength of DOM-mercury complexes<sup>19</sup> but account for a fraction of  $\text{DOS}_{\text{Red}}$  based on a mercury-titration study.<sup>34</sup> Yet, model thiols undergo rapid dark oxidation,<sup>17,18</sup> which contrasts with the dark stability of  $\text{DOS}_{\text{Red}}$  observed here. Perhaps  $\text{DOS}_{\text{Red}}$  as thiols are protected from dark oxidation by  $\text{O}_2$  in hydrophobic DOM pockets<sup>19</sup> but when exposed to sunlight rapidly oxidize due to high concentrations of photoreactive species (e.g., triplet excited state DOM ( $^3\text{CDOM}^*$ )).<sup>38</sup> This would explain the observed susceptibility of  $\text{DOS}_{\text{Red}}$  to sunlight. Although the distribution of thiol and thioethers that make up  $\text{DOS}_{\text{Red}}$  could not be resolved here, the observed complex kinetics of  $\text{DOS}_{\text{Red}}$  photochemical oxidation and previous mechanistic studies support that a combination of direct photolysis of chromophoric  $\text{DOS}_{\text{Red}}$ <sup>21</sup> and indirect photolysis via triplet excited state DOM ( $^3\text{CDOM}^*$ )<sup>22</sup> explains the photochemical oxidation of thiols and thioether groups to  $\text{SO}_4^{2-}$ .

The finding of selective  $\text{DOS}_{\text{Red}}$  photochemical oxidation to  $\text{SO}_4^{2-}$  agrees with irradiance studies of low-molecular-weight thiols and thioethers<sup>21</sup> and DOM, quantified by either the production<sup>21</sup> of  $\text{SO}_4^{2-}$  or loss of S-containing molecules.<sup>23-25</sup> Selective photochemical oxidation of  $\text{DOS}_{\text{Red}}$  to  $\text{SO}_4^{2-}$  was inferred by Ossola et al. (2019),<sup>21</sup> as this pathway was greatest in DOM collected from sulfidic environments. Further, a separate analysis presented in Figure S11 shows that the photochemical oxidation of  $\text{DOS}_{\text{Red}}$  to  $\text{SO}_4^{2-}$  measured of IHSS samples<sup>21</sup> is greatest in DOM with elevated % $\text{DOS}_{\text{Red}}$ , the latter measured by Manceau and Nagy (2012).<sup>16</sup> Photochemical oxidation of  $\text{DOS}_{\text{Red}}$  to  $\text{SO}_4^{2-}$  may occur through organic ( $\text{DOS}_{\text{SO}_2}$ ,  $\text{DOS}_{\text{SO}_3}$ ) or inorganic intermediates ( $\text{SO}_2$ ,  $\text{SO}_3^{2-}$ ),<sup>21</sup> which may not have accumulated in experimental solutions or may have been at a low concentration. It is unclear why a fraction of  $\text{DOS}_{\text{Red}}$  was photorecalcitrant (Figure 2a, Table 1), but this observation is consistent with previous laboratory studies.<sup>21,25</sup> Metals have been observed to prevent<sup>18</sup> and promote<sup>39</sup> oxidation of model reduced S compounds, but additional investigations are required with DOS. Similarly, oxidized organic S functionalities (e.g.,  $\text{DOS}_{\text{SO}_3}$ ) did not change in concentration due to irradiance. Perhaps  $\text{DOS}_{\text{SO}_3}$  groups are primarily in nonchromophoric DOM molecules, as supported by photochemical oxidation experiments of model compounds,<sup>21</sup> or that their relative low concentration obscured detection. Results from this study provide a critical atomic-level validation of mechanisms of the selective and rapid photochemical oxidation of  $\text{DOS}_{\text{Red}}$  to  $\text{SO}_4^{2-}$ .

### Implications of Findings in Biogeochemical Cycles.

The selective photochemical degradation of  $\text{DOS}_{\text{Red}}$  to  $\text{SO}_4^{2-}$  observed in DOM from sulfidic pore waters is likely an important phenomenon in fresh and marine surface waters, and is likely a result of formation<sup>1,3,9</sup> and stabilization of  $\text{DOS}_{\text{Red}}$  in DOM moieties that are highly susceptible to photochemical oxidation. The oxidation of  $\text{DOS}_{\text{Red}}$  helps explain why methylmercury (with Hg in a divalent oxidation state), exclusively bound to DOM thiols in freshwaters, is photo-reduced to gaseous elemental Hg rather than photodegraded to divalent inorganic Hg.<sup>7,8</sup>  $\text{DOS}_{\text{Red}}$  may be a precursor to minor volatile organic S species not measured here (e.g., COS,  $\text{CS}_2$ , DMS),<sup>4</sup> whereas oxidized DOS functionalities (e.g.,  $\text{DOS}_{\text{SO}_2}$ ,  $\text{DOS}_{\text{SO}_3}$ ) could be precursors of methanesulfonic acid and methanesulfonic acid;<sup>21</sup> both require future investigation. Yet, the high relative abundance of  $\text{DOS}_{\text{Red}}$  in photic freshwater systems<sup>1,16,19</sup> remains an enigma. The photostability of DOS as sulfonate ( $\text{DOS}_{\text{SO}_3}$ ) here contrasts conclusions drawn of marine and wetland DOS speciation and photolability using a molecular derivatization analysis,<sup>25,40</sup> highlighting the need for coupled atomic- and molecular-level measurements to unravel DOS complexities in natural waters. This is of particular importance in sulfur-enriched riverine and coastal environments receiving agricultural runoff<sup>41</sup> and wastewater effluent<sup>10</sup> and marine waters where DOS (de)sulfurization influences S cycling<sup>2</sup> and carbon diagenesis.<sup>14</sup> Future studies are needed to constrain  $\text{DOS}_{\text{Red}}$  speciation and quantify mechanisms and kinetics of  $\text{DOS}_{\text{Red}}$  photochemical oxidation across a variety of aquatic environments.

### ASSOCIATED CONTENT

#### Supporting Information

The Supporting Information is available free of charge at <https://pubs.acs.org/doi/10.1021/acs.estlett.3c00210>.

Description of DOM extraction, laboratory experiments, chemical analyses, and S-XANES spectra acquisition and processing (PDF)

All S-XANES spectra (XLSX)

### AUTHOR INFORMATION

#### Corresponding Author

Brett A. Poulin – Department of Environmental Toxicology, University of California Davis, Davis, California 95616, United States; [orcid.org/0000-0002-5555-7733](https://orcid.org/0000-0002-5555-7733); Phone: +1 530 754 2454; Email: [bapoulin@ucdavis.edu](mailto:bapoulin@ucdavis.edu)

Complete contact information is available at:

<https://pubs.acs.org/doi/10.1021/acs.estlett.3c00210>

#### Notes

The author declares no competing financial interest.

### ACKNOWLEDGMENTS

I thank David Krabbenhoft (USGS) (field assistance), Aron Stubbins (NU) and Sasha Wagner (RPI) (PPL extraction), Matthew Jones (CUB) and Sara Breitmeyer (USGS) (laboratory assistance), Kathryn Nagy (UIC) and Joseph Ryan (CUB) (consultation), Tianpin Wu and George Sterbinsky (APS) (beamline assistance), and 3 anonymous reviewers and William Arnold (constructive feedback). Support was provided by the U.S. Geological Survey Greater Everglades Priority Ecosystems Science (GEPES) Program and the National Science Foundation (EAR-1629698). This research used

resources of the Advanced Photon Source, a U.S. Department of Energy (DOE) Office of Science User Facility operated for the DOE Office of Science by Argonne National Laboratory under Contract No. DE-AC02-06CH11357.

## REFERENCES

- (1) Poulin, B. A.; Ryan, J. N.; Nagy, K. L.; Stubbins, A.; Dittmar, T.; Orem, W.; Krabbenhoft, D. P.; Aiken, G. R. Spatial Dependence of Reduced Sulfur in Everglades Dissolved Organic Matter Controlled by Sulfate Enrichment. *Environ. Sci. Technol.* **2017**, *51* (7), 3630–3639.
- (2) Ksionzek, K. B.; Lechtenfeld, O. J.; McCallister, S. L.; Schmitt-Kopplin, P.; Geuer, J. K.; Geibert, W.; Koch, B. P. Dissolved Organic Sulfur in the Ocean: Biogeochemistry of a Petagram Inventory. *Science* **2016**, *354* (6311), 456–459.
- (3) Vairavamurthy, A.; Mopper, K. Geochemical Formation of Organosulphur Compounds (Thiols) by Addition of H<sub>2</sub>S to Sedimentary Organic Matter. *Nature* **1987**, *329*, 623–625.
- (4) Du, Q.; Mu, Y.; Zhang, C.; Liu, J.; Zhang, Y.; Liu, C. Photochemical Production of Carbonyl Sulfide, Carbon Disulfide and Dimethyl Sulfide in a Lake Water. *J. Environ. Sci.* **2017**, *51*, 146–156.
- (5) Brigham, M. E.; Wentz, D. A.; Aiken, G. R.; Krabbenhoft, D. P. Mercury Cycling in Stream Ecosystems. I. Water Column Chemistry and Transport. *Environ. Sci. Technol.* **2009**, *43* (8), 2720–2725.
- (6) Graham, A. M.; Cameron-Burr, K. T.; Hajic, H. A.; Lee, C.; Msekela, D.; Gilmour, C. C. Sulfurization of Dissolved Organic Matter Increases Hg-Sulfide-Dissolved Organic Matter Bioavailability to a Hg-Methylating Bacterium. *Environ. Sci. Technol.* **2017**, *51* (16), 9080–9088.
- (7) Black, F. J.; Poulin, B. A.; Flegel, A. R. Factors Controlling the Abiotic Photo-Degradation of Monomethylmercury in Surface Waters. *Geochim. Cosmochim. Acta* **2012**, *84*, 492–507.
- (8) Jeremiason, J. D.; Portner, J. C.; Aiken, G. R.; Hiranaka, A. J.; Dvorak, M. T.; Tran, K. T.; Latch, D. E. Photoreduction of Hg(II) and Photodemethylation of Methylmercury: The Key Role of Thiol Sites on Dissolved Organic Matter. *Environ. Sci. Process. Impacts* **2015**, *17* (11), 1892–1903.
- (9) Hoffmann, M.; Mikutta, C.; Kretzschmar, R. Bisulfide Reaction with Natural Organic Matter Enhances Arsenite Sorption: Insights from X-Ray Absorption Spectroscopy. *Environ. Sci. Technol.* **2012**, *46* (21), 11788–11797.
- (10) Gonsior, M.; Zwartjes, M.; Cooper, W. J.; Song, W.; Ishida, K. P.; Tseng, L. Y.; Jeung, M. K.; Rosso, D.; Hertkorn, N.; Schmitt-Kopplin, P. Molecular Characterization of Effluent Organic Matter Identified by Ultrahigh Resolution Mass Spectrometry. *Water Res.* **2011**, *45* (9), 2943–2953.
- (11) Powers, L. C.; Lapham, L. L.; Malkin, S. Y.; Heyes, A.; Schmitt-Kopplin, P.; Gonsior, M. Molecular and Optical Characterization Reveals the Preservation and Sulfurization of Chemically Diverse Porewater Dissolved Organic Matter in Oligohaline and Brackish Chesapeake Bay Sediments. *Org. Geochem.* **2021**, *161*, 104324.
- (12) Sleighter, R. L.; Chin, Y.-P.; Arnold, W. A.; Hatcher, P. G.; McCabe, A. J.; McAdams, B. C.; Wallace, G. C. Evidence of Incorporation of Abiotic S and N into Prairie Wetland Dissolved Organic Matter. *Environ. Sci. Technol. Lett.* **2014**, *1* (9), 345–350.
- (13) Gomez-Saez, G. V.; Dittmar, T.; Holtappels, M.; Pohlbeln, A. M.; Lichtschlag, A.; Schnetger, B.; Boetius, A.; Niggemann, J. Sulfurization of Dissolved Organic Matter in the Anoxic Water Column of the Black Sea. *Sci. Adv.* **2021**, *7* (25), No. eabf6199.
- (14) Raven, M. R.; Keil, R. G.; Webb, S. M. Microbial Sulfate Reduction and Organic Sulfur Formation in Sinking Marine Particles. *Science* **2021**, *371* (6525), 178–181.
- (15) Gomez-Saez, G. V.; Niggemann, J.; Dittmar, T.; Pohlbeln, A. M.; Lang, S. Q.; Noowong, A.; Pichler, T.; Wörmer, L.; Bühring, S. I. Molecular Evidence for Abiotic Sulfurization of Dissolved Organic Matter in Marine Shallow Hydrothermal Systems. *Geochim. Cosmochim. Acta* **2016**, *190*, 35–52.
- (16) Manceau, A.; Nagy, K. L. Quantitative Analysis of Sulfur Functional Groups in Natural Organic Matter by XANES Spectroscopy. *Geochim. Cosmochim. Acta* **2012**, *99*, 206–223.
- (17) Chu, C.; Erickson, P. R.; Lundeen, R. a.; Stamatielatos, D.; Alaimo, P. J.; Latch, D. E.; McNeill, K. Photochemical and Nonphotochemical Transformations of Cysteine with Dissolved Organic Matter. *Environ. Sci. Technol.* **2016**, *50* (12), 6363–6373.
- (18) Hsu-Kim, H. Stability of Metal-Glutathione Complexes during Oxidation by Hydrogen Peroxide and Cu(II)-Catalysis. *Environ. Sci. Technol.* **2007**, *41* (7), 2338–2342.
- (19) Haitzer, M.; Aiken, G. R.; Ryan, J. N. Binding of Mercury(II) to Aquatic Humic Substances: Influence of PH and Source of Humic Substances. *Environ. Sci. Technol.* **2003**, *37* (11), 2436–2441.
- (20) Liem-Nguyen, V.; Skyllberg, U.; Björn, E. Thermodynamic Modeling of the Solubility and Chemical Speciation of Mercury and Methylmercury Driven by Organic Thiols and Micromolar Sulfide Concentrations in Boreal Wetland Soils. *Environ. Sci. Technol.* **2017**, *51* (7), 3678–3686.
- (21) Ossola, R.; Tolu, J.; Clerc, B.; Erickson, P. R.; Winkel, L. H. E.; McNeill, K. Photochemical Production of Sulfate and Methanesulfonic Acid from Dissolved Organic Sulfur. *Environ. Sci. Technol.* **2019**, *53* (22), 13191–13200.
- (22) Ossola, R.; Clerc, B.; McNeill, K. Mechanistic Insights into Dissolved Organic Sulfur Photomineralization through the Study of Cysteine Sulfinic Acid. *Environ. Sci. Technol.* **2020**, *54* (20), 13066–13076.
- (23) Stubbins, A.; Spencer, R. G. M.; Chen, H.; Hatcher, P. G.; Mopper, K.; Hernes, P. J.; Mwamba, V. L.; Mangangu, A. M.; Wabakanghanzi, J. N.; Six, J. Illuminated Darkness: Molecular Signatures of Congo River Dissolved Organic Matter and Its Photochemical Alteration as Revealed by Ultrahigh Precision Mass Spectrometry. *Limnol. Oceanogr.* **2010**, *55* (4), 1467–1477.
- (24) Herzsprung, P.; Hertkorn, N.; Friese, K.; Schmitt-Kopplin, P. Photochemical Degradation of Natural Organic Sulfur Compounds (CHOS) from Iron-Rich Mine Pit Lake Pore Waters-An Initial Understanding from Evaluation of Single-Elemental Formulae Using Ultra-High-Resolution Mass Spectrometry. *Rapid Commun. Mass Spectrom.* **2010**, *24* (19), 2909–2924.
- (25) Gomez-Saez, G. V.; Pohlbeln, A. M.; Stubbins, A.; Marsay, C. M.; Dittmar, T. Photochemical Alteration of Dissolved Organic Sulfur from Sulfidic Porewater. *Environ. Sci. Technol.* **2017**, *51* (24), 14144–14154.
- (26) Tate, M. T.; DeWild, J. F.; Ogorek, J. M.; Janssen, S. E.; Krabbenhoft, D. P.; Poulin, B. A.; Breitmeyer, S. E.; Aiken, G. R.; Orem, W. H.; Varonka, M. S. Chemical Characterization of Water, Sediments, and Fish from Water Conservation Areas and Canals of the Florida Everglades (USA), 2012 to 2019. *U.S. Geologic Survey data release 2023*, DOI: 10.5066/P976EGIX.
- (27) Aiken, G. R.; McKnight, D. M.; Thorn, K. A.; Thurman, E. M. Isolation of Hydrophilic Organic Acids from Water Using Nonionic Macroporous Resins. *Org. Geochem.* **1992**, *18* (4), 567–573.
- (28) Dittmar, T.; Koch, B.; Hertkorn, N.; Kattner, G. A Simple and Efficient Method for the Solid-Phase Extraction of Dissolved Organic Matter (SPE-DOM) from Seawater. *Limnol. Oceanogr. Methods* **2008**, *6* (6), 230–235.
- (29) Sharpless, C. M.; Aeschbacher, M.; Page, S. E.; Wenk, J.; Sander, M.; McNeill, K. Photooxidation-Induced Changes in Optical, Electrochemical, and Photochemical Properties of Humic Substances. *Environ. Sci. Technol.* **2014**, *48* (5), 2688–2696.
- (30) Weishaar, J. L.; Aiken, G. R.; Bergamaschi, B. a.; Fram, M. S.; Fujii, R.; Mopper, K. Evaluation of Specific Ultraviolet Absorbance as an Indicator of the Chemical Composition and Reactivity of Dissolved Organic Carbon. *Environ. Sci. Technol.* **2003**, *37* (20), 4702–4708.
- (31) Helms, J. R.; Stubbins, A.; Ritchie, J. D.; Minor, E. C.; Kieber, D. J.; Mopper, K. Absorption Spectral Slopes and Slope Ratios as Indicators of Molecular Weight, Source, and Photobleaching of Chromophoric Dissolved Organic Matter. *Limnol. Oceanogr.* **2008**, *53* (3), 955–969.

- (32) Ohno, T. Fluorescence Inner-Filtering Correction for Determining the Humification Index of Dissolved Organic Matter. *Environ. Sci. Technol.* **2002**, *36* (4), 742–746.
- (33) Hansen, A. M.; Kraus, T. E. C.; Pellerin, B. A.; Fleck, J. A.; Downing, B. D.; Bergamaschi, B. A. Optical Properties of Dissolved Organic Matter (DOM): Effects of Biological and Photolytic Degradation. *Limnol. Oceanogr.* **2016**, *61* (3), 1015–1032.
- (34) Haitzer, M.; Aiken, G. R.; Ryan, J. N. Binding of Mercury(II) to Dissolved Organic Matter: The Role of the Mercury-to-DM Concentration Ratio. *Environ. Sci. Technol.* **2002**, *36* (16), 3564–3570.
- (35) Pierce, C. E.; Furman, O. S.; Nicholas, S. L.; Wasik, J. C.; Gionfriddo, C. M.; Wymore, A. M.; Sebestyen, S. D.; Kolka, R. K.; Mitchell, C. P. J.; Griffiths, N. A.; Elias, D. A.; Nater, E. A.; Toner, B. M. Role of Ester Sulfate and Organic Disulfide in Mercury Methylation in Peatland Soils. *Environ. Sci. Technol.* **2022**, *56* (2), 1433–1444.
- (36) Maurer, F.; Christl, I.; Hoffmann, M.; Kretzschmar, R. Reduction and Reoxidation of Humic Acid: Influence on Speciation of Cadmium and Silver. *Environ. Sci. Technol.* **2012**, *46* (16), 8808–8816.
- (37) Manceau, A.; Lemouchi, C.; Rovezzi, M.; Lanson, M.; Glatzel, P.; Nagy, K. L.; Gautier-Luneau, I.; Joly, Y.; Enescu, M. Structure, Bonding, and Stability of Mercury Complexes with Thiolate and Thioether Ligands from High-Resolution XANES Spectroscopy and First-Principles Calculations. *Inorg. Chem.* **2015**, *54* (24), 11776–11791.
- (38) Latch, D. E.; McNeill, K. Microheterogeneity of Singlet Oxygen Distributions in Irradiated Humic Acid Solutions. *Science* **2006**, *311* (5768), 1743–1747.
- (39) Chu, C.; Stamatelatos, D.; McNeill, K. Aquatic Indirect Photochemical Transformations of Natural Peptidic Thiols: Impact of Thiol Properties, Solution PH, Solution Salinity and Metal Ions. *Environ. Sci. Process. Impacts* **2017**, *19* (12), 1518–1527.
- (40) Pohlbeln, A. M.; Gomez-Saez, G. V.; Noriega-Ortega, B. E.; Dittmar, T. Experimental Evidence for Abiotic Sulfurization of Marine Dissolved Organic Matter. *Front. Mar. Sci.* **2017**, *4*, 364.
- (41) Hinckley, E.-L. S.; Crawford, J. T.; Fakhraei, H.; Driscoll, C. T. A Shift in Sulfur-Cycle Manipulation from Atmospheric Emissions to Agricultural Additions. *Nat. Geosci.* **2020**, *13* (9), 597–604.